PAXX and XLF DNA repair factors are functionally redundant in joining DNA breaks in a G1-arrested progenitor B-cell line

Vipul Kumar[a,b,c,1], Frederick W. Alt[a,b,c,2], and Richard L. Frock[a,b,c,1]

[a]Howard Hughes Medical Institute, Boston, MA 02115; [b]Program in Cellular and Molecular Medicine, Boston Children's Hospital, Boston, MA 02115; and [c]Department of Genetics, Harvard Medical School, Boston, MA 02115

Contributed by Frederick W. Alt, July 21, 2016 (sent for review June 28, 2016; reviewed by Jayanta Chaudhuri, JoAnn M. Sekiguchi, and Kefei Yu)

Classical nonhomologous end joining (C-NHEJ) is a major mammalian DNA double-strand break (DSB) repair pathway. Core C-NHEJ factors, such as XRCC4, are required for joining DSB intermediates of the G1 phase-specific V(D)J recombination reaction in progenitor lymphocytes. Core factors also contribute to joining DSBs in cycling mature B-lineage cells, including DSBs generated during antibody class switch recombination (CSR) and DSBs generated by ionizing radiation. The XRCC4-like-factor (XLF) C-NHEJ protein is dispensable for V(D)J recombination in normal cells, but because of functional redundancy, it is absolutely required for this process in cells deficient for the ataxia telangiectasia-mutated (ATM) DSB response factor. The recently identified paralogue of XRCC4 and XLF (PAXX) factor has homology to these two proteins and variably contributes to ionizing radiation-induced DSB repair in human and chicken cells. We now report that PAXX is dispensable for joining V(D)J recombination DSBs in G1-arrested mouse pro-B–cell lines, dispensable for joining CSR-associated DSBs in a cycling mouse B-cell line, and dispensable for normal ionizing radiation resistance in both G1-arrested and cycling pro-B lines. However, we find that combined deficiency for PAXX and XLF in G1-arrested pro-B lines abrogates DSB joining during V(D)J recombination and sensitizes the cells to ionizing radiation exposure. Thus, PAXX provides core C-NHEJ factor-associated functions in the absence of XLF and vice versa in G1-arrested pro–B-cell lines. Finally, we also find that PAXX deficiency has no impact on V(D)J recombination DSB joining in ATM-deficient pro-B lines. We discuss implications of these findings with respect to potential PAXX and XLF functions in C-NHEJ.

C-NHEJ | PAXX | XLF | V(D)J recombination | DNA repair

To repair DNA double-strand breaks (DSBs), mammalian cells use two major DSB repair pathways: homologous recombination (HR) and classical nonhomologous end joining (C-NHEJ). HR requires a long homologous template for repair and is active in S/G2 cell cycle phase (1). In contrast, C-NHEJ, which directly ligates DSBs with short (1–4 bp) or no homologies, functions throughout interphase, including during the G1 cell cycle phase (2–4). C-NHEJ repairs diverse DSBs, including those arising ectopically by ionizing radiation as well as DSBs generated as intermediates during V(D)J recombination in developing progenitor (pro)-B and -T lymphocytes and Ig heavy chain (IgH) class switch recombination (CSR) in activated mature B lymphocytes (5). The C-NHEJ pathway has a number of characterized members, including "core" C-NHEJ factors that were so-named in part based on their requirement for joining known types of ends via C-NHEJ and their evolutionary conservation (6). Such core factors include the Ku70 and Ku80 proteins, which form the "Ku" end recognition complex, and the XRCC4 and DNA Ligase4 proteins, which form the C-NHEJ ligation complex (5, 6).

Exons that encode Ig and T-cell receptor (TCR) variable region exons are assembled from germline V, D, and J gene segments. This V(D)J recombination process, which takes place in pro-B and -T lymphocytes, occurs within the G1 cell cycle phase (7). Each V(D)J gene segment is flanked by a recombination signal sequence (RSS) that is a target of the RAG1/2 (RAG) endonuclease. RAG generates DSBs precisely between the RSS and flanking coding gene segment to create hair-pinned coding ends (CEs) and blunt, 5′-phosphorylated RSS ends (also termed signal ends) (8). Subsequently, the joining of both CEs and signal ends during V(D)J recombination is absolutely dependent on core C-NHEJ factors (5). Mice lacking any core C-NHEJ component cannot assemble antigen receptor variable region exons and correspondingly, have SCID that manifests as complete lack of mature B and T cells (6).

Activated cycling mature B cells use CSR to exchange their initially expressed IgM heavy-chain constant (Cμ) region exons for a set of downstream exons (e.g., Cγ, Cε, Cα, etc.) that encodes a different *IgH* Cμ region and antibody effector functions. CSR is a cut and paste process that is initiated specifically by activation-induced cytidine deaminase (AID) (9). In this regard, the various sets of CH exons are each flanked upstream by long repetitive switch (S) regions. During CSR, AID introduces deamination lesions into Sμ and a targeted downstream acceptor S region. Subsequently, these S region deamination lesions are converted into DSBs that are end joined to fuse Sμ and a downstream S region to complete CSR (5). Notably, whereas core C-NHEJ likely contributes substantially to end joining during CSR, in their absence, this reaction can be mediated at nearly 50% of WT levels by alternative end joining (A-EJ) pathways. A-EJ tends to more frequently use microhomologies

Significance

Classical nonhomologous end joining (C-NHEJ) is a major mammalian DNA double–strand break (DSB) repair pathway. During V(D)J recombination in progenitor (pro)-B lymphocytes, C-NHEJ joins programmed DSBs in antibody gene loci to form complete antibody genes. C-NHEJ also protects mammalian cells from the harmful effects of exposure to ionizing radiation. We now find that the recently identified paralogue of XRCC4 and XLF (PAXX) DNA repair factor, like the related XLF repair factor, is dispensable for V(D)J recombination. However, combined loss of these two factors in pro–B-cell lines totally abrogates V(D)J recombination DSB joining and greatly sensitizes the cells to ionizing radiation. These findings show that PAXX can provide critical C-NHEJ functions that are normally masked by functional redundancy with XLF.

Author contributions: V.K., F.W.A., and R.L.F. designed research; V.K. and R.L.F. performed research; V.K., F.W.A., and R.L.F. analyzed data; and V.K., F.W.A., and R.L.F. wrote the paper.

Reviewers: J.C., Memorial Sloan Kettering Cancer Center; J.M.S., University of Michigan; and K.Y., Michigan State University.

The authors declare no conflict of interest.

Data deposition: The data reported in this paper have been deposited in the Gene Expression Omnibus (GEO) database, www.ncbi.nlm.nih.gov/geo (accession no. GSE84102).

[1]V.K. and R.L.F. contributed equally to this work.

[2]To whom correspondence should be addressed. Email: alt@enders.tch.harvard.edu.

This article contains supporting information online at www.pnas.org/lookup/suppl/doi:10.1073/pnas.1611882113/-/DCSupplemental.

(MHs) than C-NHEJ during CSR (10). A-EJ also substantially contributes to joining other types of DSBs in core C-NHEJ–deficient cycling cells (11, 12).

There are various C-NHEJ factors that are not required as broadly as core factors. In this regard, absence of either DNA-dependent protein kinase catalytic subunit (DNA-PKcs) or Artemis abrogates V(D)J CE joining, at least in part because of the role of these factors in hairpin opening and processing, but has much less impact on signal end joining (13). Functional redundancies with other factors can also impact on the requirement for certain C-NHEJ factors with respect to joining various classes of DSBs (6). For example, XLF deficiency has no measurable impact on chromosomal V(D)J recombination (14, 15) because of functional redundancy with the ataxia telangiectasia-mutated (ATM) DNA DSB response (DSBR) protein (6). Thus, although ATM deficiency only mildly impacts V(D)J recombination, this process is abrogated in developing pro-B cells dually deficient for XLF and ATM or downstream DSB response factors (16–18). XLF also is functionally redundant with DNA-PKcs in V(D)J recombination signal end joining (19). Potential processes in which XLF and DSBR factors may be functionally redundant are not well-characterized but may include tethering ends or facilitating their joining (6, 16). Notably, XLF also has functional redundancy with a truncation mutant of RAG2 for CE joining during V(D)J recombination, potentially implicating the RAG2 protein in some aspect of shepherding the V(D)J recombination joining reaction specifically to C-NHEJ (20, 21).

The paralogue of XRCC4 and XLF (PAXX; also known as c9ORF142 and XRCC4-like small protein) recently has been implicated as a C-NHEJ factor based on its structural similarity to XRCC4 and XLF (22–24). In this regard, PAXX deficiency conferred a range of ionizing radiation sensitivity in various human or chicken cell lines. In addition, although XLF deficiency modestly impacts V(D)J joining in extrachromosomal substrates in nonlymphoid cells (14), PAXX deficiency has been found to accentuate the requirement for XLF for this process (25). To further elucidate PAXX function in C-NHEJ, we now have assayed for potential unique roles of PAXX and potential functionally redundant roles of PAXX with XLF.

Results

PAXX Is Dispensable for End Joining During V(D)J Recombination. To elucidate PAXX functions in C-NHEJ during V(D)J recombination, we used CRISPR-Cas9 to delete the entire ORF of murine *PAXX* in a previously characterized WT *bcl-2* transgenic *v-Abl* kinase-transformed pro–B-cell line (16) (hereafter referred to as *v-Abl* cells) (Fig. S1 *A* and *B*) and assayed two independent clones of PAXX$^{-/-}$ *v-Abl* cells. Treatment of *v-Abl* lines with *Abl* kinase inhibitor STI-571 leads to G1 arrest, induction of RAG1/RAG2 protein expression, and V(D)J recombination at endogenous RAG target loci as well as chromosomally integrated reporter substrates. The *bcl-2* transgene circumvents STI-571–induced apoptosis to allow analysis of induced V(D)J recombination (26). Using the same Southern blot probe, coding joins (CJs) and unrepaired CEs can be measured in cells containing either the pMX-DEL-CJ or pMX-INV substrates, whereas signal joins (SJs) and unrepaired signal ends can be measured in cells containing pMX-DEL-SJ substrates (26) (Fig. 1*A* and Fig. S2 *A* and *C*). Based on assays with these three chromosomally integrated substrates, as expected, STI-571–treated WT *v-Abl* cells accumulated a substantial fraction of CJs and SJs with no detectable CEs and signal ends, whereas STI-571–treated XLF$^{-/-}$ ATM$^{-/-}$ and Ligase4$^{-/-}$ *v-Abl* cells accumulated unrepaired CEs and signal ends in the absence of readily detectable CJs or SJs. In both PAXX$^{-/-}$ clones, assays of both types of integrated CJ/CE substrates and the SJ/signal end substrate revealed WT levels of CJ and SJ formation with no detectable evidence of CEs or signal ends (Fig. 1*B* and Fig. S2 *B*, *D*, and *E*). We conclude that PAXX is dispensable for repair of CEs and signal ends during V(D)J recombination within chromosomal V(D)J recombination substrates.

PAXX Contributes to Core C-NHEJ During V(D)J Recombination in the Absence of XLF but Not in the Absence of ATM. The lack of detectable impact of PAXX deficiency on V(D)J recombination indicates either that PAXX is dispensable for this process or that PAXX functions can be compensated for by other factors. Given the structural similarity shared between PAXX, XRCC4, and XLF (22, 23), we hypothesized that potential functions of PAXX in V(D)J recombination might be masked by functional redundancies with XLF or the ATM-dependent DSBR. To test this hypothesis, we generated two separate clones of XLF$^{-/-}$PAXX$^{-/-}$ and two clones of ATM$^{-/-}$PAXX$^{-/-}$ *v-Abl* cells from XLF$^{-/-}$ and ATM$^{-/-}$ parental *v-Abl* lines (Fig. S1 *A* and *B*) and performed V(D)J recombination substrate analyses as described above for PAXX$^{-/-}$ *v-Abl* lines. Consistent with prior observations (26), ATM$^{-/-}$ *v-Abl* cells accumulated CJs and a fraction of unrepaired CEs with both tested substrates and generated SJs without detectable unrepaired signal ends (Fig. 2 *A* and *B* and Fig. S3). Likewise, both clones of ATM$^{-/-}$PAXX$^{-/-}$ *v-Abl* cells accumulated CJs, CEs, and SJs similarly to ATM$^{-/-}$ cells (Fig. 2*A* and Fig. S3). Thus, there seems to be little or no functional overlap between ATM and PAXX with respect to V(D)J recombination.

As expected (14, 20), XLF$^{-/-}$ *v-Abl* cells assayed with both CJ substrates showed a largely normal accumulation of CJs, with very minor levels of unrepaired CEs (Fig. 2 *A* and *B* and Fig. S3), and when assayed for SJs, they also showed profiles that appear largely normal (Fig. 2*B*). Strikingly, however, both clones of XLF$^{-/-}$PAXX$^{-/-}$ *v-Abl* cells as assayed with both CJ constructs and the SJ construct showed a complete absence of CJs and SJs and a

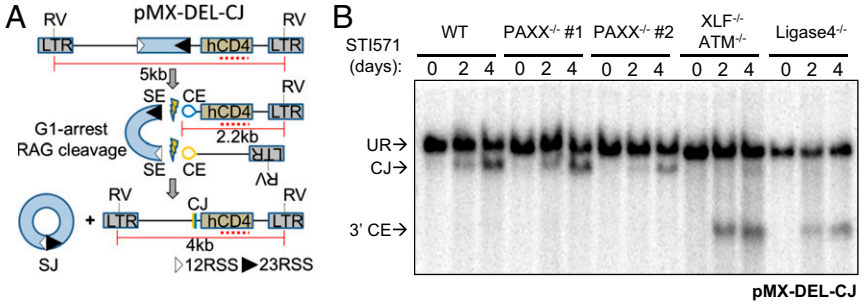

Fig. 1. PAXX deficiency does not affect coding joining during V(D)J recombination. (*A*) Overview of the pMX-DEL-CJ retroviral construct. The 12RSS and 23RSS are convergently oriented to monitor deletional CJs via Southern blotting assays. The CD4 probe (red dashed lines) combined with EcoRV-digested genomic DNA reveal germline unrearranged fragments (URs), CJs, and free CEs. LTR, viral long-terminal repeat; RV, EcoRV; SE, signal end. (*B*) Southern blot analysis of CJs and CEs for WT, PAXX$^{-/-}$, and Ligase4$^{-/-}$ *v-Abl* cells. Numbers 1 and 2 indicate independent clones assayed for a given genotype.

corresponding accumulation of CEs and signal ends (Fig. 2 *A* and *B* and Fig. S3). Indeed, the defect in V(D)J recombination CE and signal end joining appeared as severe as that of similarly treated XLF$^{-/-}$ATM$^{-/-}$ or Ligase4$^{-/-}$ *v-Abl* lines (Fig. 2 *A* and *B* and Fig. S3). To confirm that the inactivation of PAXX in XLF$^{-/-}$ *v-Abl* cells was, indeed, the cause of this dramatic end joining defect, we retrovirally complemented both of the XLF$^{-/-}$PAXX$^{-/-}$ clones with either PAXX or XLF and found that ectopic expression of either of these factors was sufficient to restore both CE and signal end joining to XLF$^{-/-}$ or PAXX$^{-/-}$ levels, respectively (Fig. 2 *C* and *D* and Fig. S4). These findings indicate that PAXX and XLF serve functionally redundant roles in core C-NHEJ during V(D)J recombination.

PAXX Is Dispensable for CSR C-NHEJ in the Presence or Absence of XLF. To determine whether PAXX deficiency, either alone or in the absence of XLF, affects end joining of DNA DSBs beyond those associated with V(D)J recombination, we tested the impact of PAXX deficiency on *IgH* CSR. The CH12F3 (CH12) B-cell lymphoma cell line can be induced in culture to undergo robust CSR to IgA by treatment with a combination of anti-CD40, IL-4, and TGF-β (27). For these analyses, we used a Cas9/guide-RNA (gRNA) approach to generate independent lines of PAXX$^{-/-}$, XLF$^{-/-}$, and XLF$^{-/-}$PAXX$^{-/-}$ CH12 cells (Fig. S5 *A* and *B*). PAXX$^{-/-}$ CH12 cells underwent CSR to IgA at levels comparable with those of the parental WT CH12 line (average: 55 and 65% for PAXX$^{-/-}$ vs. 50 and 62% for WT cells on days 2 and 3 of stimulation, respectively) (Fig. 3*A* and Fig. S6). Consistent with studies of CSR to IgG1 in XLF$^{-/-}$ primary B cells (14), XLF$^{-/-}$ CH12 cells underwent CSR to IgA at about 32 and 39% of WT levels on days 2 and 3 of stimulation, respectively. This level of *IgH* class switching was very similar to that of CH12 cells deficient for the core C-NHEJ factor Ligase4 (Fig. 3*A* and Figs. S5 *C* and *D* and S6). In the latter context, XLF$^{-/-}$PAXX$^{-/-}$ CH12 cells, perhaps not surprisingly, showed no obvious impairment in CSR to IgA beyond that observed for XLF$^{-/-}$ CH12 cells (Fig. 3*A* and Fig. S6).

Minor effects of C-NHEJ deficiencies on *IgH* CSR cannot, in some cases, be readily apparent to assays that measure *IgH* class switching by surface staining. For example, Artemis deficiency has little or no impact on IgM to IgG1 switching relative to WT as measured by surface staining but does have an impact on CSR that can be observed via an FISH assay to quantify levels of unrepaired *IgH CH* locus breaks. In addition, this assay directly indicates end joining defects as opposed to the surface staining assay that measures impacts on CSR that could occur at various levels (28, 29). Thus, we used *IgH* FISH to look for *IgH* chromosomal breaks (and translocations) in CSR-activated WT and mutant CH12 cells after 2 d of activation for IgA class switching. In these studies, the levels of chromosomal *IgH* breaks were not distinguishable between activated WT and PAXX$^{-/-}$ CH12 cells (~2% in both) (Fig. 3*B*). In contrast, CSR-activated XLF$^{-/-}$ CH12 cells showed a marked increase in chromosomal breaks that was not significantly increased in XLF$^{-/-}$PAXX$^{-/-}$ CH12 cells (about 10% in both genotypes) (Fig. 3*B*). Notably, the level of chromosomal breaks in Ligase4$^{-/-}$ CH12 cells (25%) (Fig. 3*B*) was much greater than that of XLF$^{-/-}$ CH12 cells (Fig. 3*B*). Additional work will be needed to understand why relative levels of *IgH* breaks are greater in Ligase4$^{-/-}$ CH12 cells relative to XLF$^{-/-}$ CH12 cells given their very similarly reduced levels of IgA class switching. We note, however, that mechanisms for this type of divergence that do not necessarily relate to the CSR mechanism per se have been implicated in different CSR stimulation conditions and other factors (29, 30).

Prior studies of limited numbers of CSR junctions indicate that more than 90% of CSR joins in core C-NHEJ factor-deficient activated B cells are not direct and use MHs as opposed to those from WT B cells that generally have a much larger fraction of direct junctions (31–33). To assess the structure of a large number of Sμ to Sα CSR junctions from the various WT and mutant CH12 cells after 3 d of activation, we used our recently developed high-throughput CSR junction assay (30). Based on analysis of thousands of CSR junctions from WT and PAXX$^{-/-}$ CH12 cells (Table S1), we observed no significant difference in use of junctional MHs, with nearly 25% of junctions being direct and an overall mean MH length of ~1.8 bp in both cell types (Fig. 3 *C* and *D* and Table S1). Consistent with prior observations of MH bias in Sμ-Sγ1 junctions in XLF$^{-/-}$ primary B cells (14), analysis of thousands of

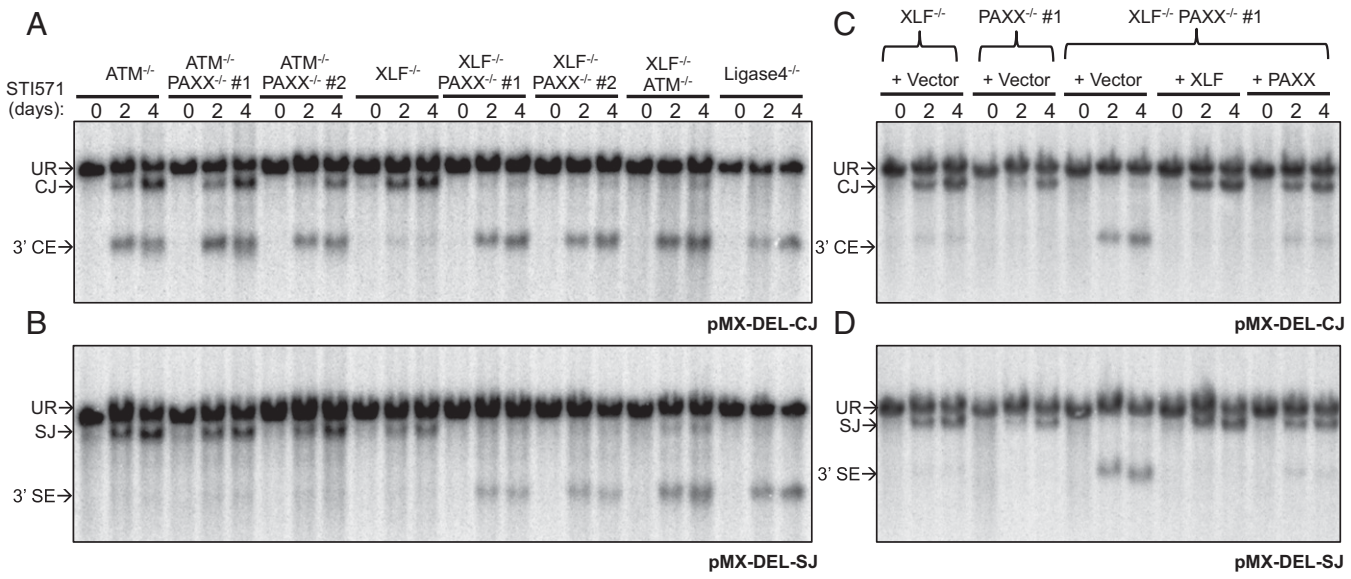

Fig. 2. XLF$^{-/-}$PAXX$^{-/-}$ but not ATM$^{-/-}$PAXX$^{-/-}$ *v-Abl* cells are abrogated for coding and signal end joining block during V(D)J recombination. Southern analysis of CJs and SJs from (*A*) pMX-DEL-CJ or (*B*) pMX-DEL-SJ containing ATM$^{-/-}$, ATM$^{-/-}$PAXX$^{-/-}$, XLF$^{-/-}$, XLF$^{-/-}$PAXX$^{-/-}$, and Ligase4$^{-/-}$ *v-Abl* cells. Southern analysis of the (*C*) pMX-DEL-CJ or (*D*) pMX-DEL-SJ recombination substrates in XLF$^{-/-}$PAXX$^{-/-}$ *v-Abl* clone 1 complemented with empty vector, XLF, or PAXX compared with XLF$^{-/-}$ and PAXX$^{-/-}$ 1 *v-Abl* lines transduced with empty vector. Complementation results for XLF$^{-/-}$PAXX$^{-/-}$ 2 are shown in Fig. S4. SE, signal end; UR, unrearranged fragment.

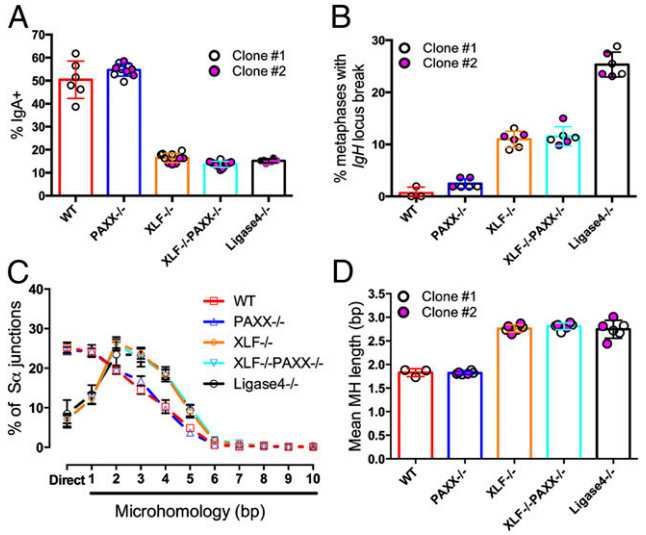

Fig. 3. PAXX deficiency does not affect end joining during CSR. (*A*) IgA staining quantified by flow cytometry for WT, PAXX$^{-/-}$, XLF$^{-/-}$, XLF$^{-/-}$PAXX$^{-/-}$, and Ligase4$^{-/-}$ CH12 B cells stimulated for CSR on day 2. Fig. S6*A* shows CSR analysis on day 3. (*B*) Metaphase FISH analysis for *IgH* locus breaks of stimulated WT, PAXX$^{-/-}$, XLF$^{-/-}$, XLF$^{-/-}$PAXX$^{-/-}$, and Ligase4$^{-/-}$ CH12 cells from day 2 stimulated CH12 cells; 50–60 metaphases were analyzed for each replicate across all clones. (*C*) Junction structure distributions between Sμ and Sα for WT (red square), PAXX$^{-/-}$ (blue triangle), XLF$^{-/-}$ (orange diamond), XLF$^{-/-}$PAXX$^{-/-}$ (light blue downward triangle), and Ligase4$^{-/-}$ (black circle) CH12 cells as determined by linear amplification-mediated high-throughput genome-wide translocation sequencing (LAM-HTGTS) assay (30) from day 3 stimulated CH12 cells (n = 3 for each clone). Table S1 shows individual clone distributions. (*D*) Mean MH lengths are reported for WT, PAXX$^{-/-}$, XLF$^{-/-}$, XLF$^{-/-}$PAXX$^{-/-}$, and Ligase4$^{-/-}$ CH12 cells. (*A*, *B*, and *D*) All graphs are displayed as means ± SD. Clones 1 and 2 are indicated for each genotype by white and purple circles, respectively; $n \geq 3$ independent stimulations for each clone.

junctions from XLF$^{-/-}$ CH12 cells revealed a profound MH bias, with only ∼7% of junctions using direct joins and an overall mean MH length of 2.8 bp (Fig. 3 *C* and *D* and Table S1). Indeed, the shift from direct to MH-mediated junctions was indistinguishable from that observed for Ligase4-deficient CH12 cells (Fig. 3*A*), consistent with the similar impact of XLF and this core C-NHEJ factor on *IgH* class switching as measured by the FACS surface staining assay. In this context, loss of PAXX did not impact the MH bias in either direction beyond the severe effect found for XLF deficiency, because analysis of thousands of CSR junctions from XLF$^{-/-}$PAXX$^{-/-}$ CH12 cells showed ∼7% direct join use and a mean MH length of 2.8 bp (Fig. 3 *C* and *D* and Table S1).

PAXX and XLF Are Functionally Redundant for Repair of Ionizing Radiation-Induced DSBs in G1 Phase-Enriched *v-Abl* Lines. To test for potential roles of PAXX, in either the presence or the absence of XLF, in the repair of more general DSBs, we assayed cycling WT and the various mutant CH12 cells for ionizing radiation sensitivity. These assays revealed that PAXX$^{-/-}$ CH12 cells did not detectably exhibit ionizing radiation sensitivity beyond that of WT CH12 cells (Fig. 4*A*), indicating that PAXX is dispensable for the repair of this general class of DSBs in CH12 cells. However, XLF$^{-/-}$ cycling CH12 cells revealed ionizing radiation sensitivity that was clearly greater than that of WT but in contrast to their CSR defect, not as severe as that of Ligase4$^{-/-}$ CH12 cells (Fig. 4*A*). Moreover, with respect to ionizing radiation sensitivity, XLF$^{-/-}$PAXX$^{-/-}$ CH12 cells showed no greater sensitivity to ionizing radiation than that of XLF$^{-/-}$ cells alone (Fig. 4*A*). We conclude that PAXX has no major functional redundancy with XLF with respect to sensitivity to ionizing radiation-induced DNA damage in cycling CH12 cells.

Our finding that the functional redundancy of PAXX and XLF with respect to V(D)J recombination in G1-phase *v-Abl* lines does not extend to ionizing radiation sensitivity in cycling CH12 cells might reflect cell type and stage differences. To test this possibility, we used clonogenic survival assays to test ionizing radiation sensitivity of the various WT and mutant *v-Abl* transformed lines that were ionizing radiation treated while cycling. As expected for core C-NHEJ deficiency (14), the survival of cycling Ku70$^{-/-}$ *v-Abl* cells was profoundly inhibited by ionizing radiation treatment compared with that of ionizing radiation-treated WT cells (Fig. 4*B*). In contrast, cycling PAXX$^{-/-}$ *v-Abl* cells exhibited no detectable ionizing radiation sensitivity compared with WT, a result consistent with the dispensability of PAXX for V(D)J recombination, CSR, and ionizing radiation resistance in cycling CH12 cells. As also expected (14), cycling XLF$^{-/-}$ *v-Abl* cells exhibited intermediate ionizing radiation sensitivity relative to WT and Ku70$^{-/-}$ *v-Abl* cells (Fig. 4*B*). However, cycling XLF$^{-/-}$PAXX$^{-/-}$ cells did not exhibit ionizing radiation sensitivity beyond that of XLF$^{-/-}$ cells (Fig. 4*B*). We conclude that neither cycling CH12 cells nor cycling *v-Abl* cells show functional redundancy of PAXX and XLF for repair of ionizing radiation-induced DSBs.

The are several possible explanations for the apparent discrepancy between the functional redundancy observed for PAXX and XLF in V(D)J recombination in G1-arrested *v-Abl* cells and the absence of functional redundancy in mediating ionizing radiation resistance in cycling *v-Abl* and CH12 cells. One possibility would be that this functional redundancy only occurs in the context of DSB repair during V(D)J recombination. Alternatively, the functional redundancy of these two factors might apply more broadly to DSB repair but would only be manifested for DSBs that are generated in the G1 cell cycle phase. To distinguish between these two possibilities, we treated v-*Abl* lines with ionizing radiation, when they were G1 arrested via STI-571 treatment (Fig. S7), and then, we subsequently released them into cycle to perform clonogenic survival assays (*Materials and Methods*). Based on this assay, G1-arrested Ku70$^{-/-}$ cells were extremely sensitive to ionizing radiation treatment compared with WT *v-Abl* cells, whereas G1-arrested PAXX$^{-/-}$ *v-Abl* cells had ionizing radiation sensitivity indistinguishable from that of WT (Fig. 4*C*). G1-arrested XLF$^{-/-}$ *v-Abl* cells had an intermediate level of ionizing radiation sensitivity compared with WT and Ku70$^{-/-}$ counterparts, but strikingly, G1-arrested XLF$^{-/-}$PAXX$^{-/-}$ *v-Abl* cells also were extremely ionizing radiation sensitive relative to XLF$^{-/-}$ or PAXX$^{-/-}$ G1-arrested *v-Abl* cells (Fig. 4*C*). However, we could not directly compare the ionizing radiation sensitivity between Ku70$^{-/-}$ and XLF$^{-/-}$PAXX$^{-/-}$ *v-Abl* cells, because in both cases, clonogenic survival under these conditions was beyond the sensitivity of our current assays (Fig. 4*C*). Finally, we note that the extreme ionizing radiation hypersensitivity of XLF$^{-/-}$PAXX$^{-/-}$ *v-Abl* cells revealed by these experiments was rescued to levels observed in PAXX$^{-/-}$ or XLF$^{-/-}$ cells by complementation via ectopic expression of either XLF or PAXX, respectively (Fig. 4*C* and Fig. S1 *C* and *D*). These findings indicate that PAXX and XLF have functional redundancy for repair of ionizing radiation-induced DSBs generated in G1-phase *v-Abl* cells.

We considered the possibility that the functional redundancy that we observed in STI-571–treated *v-Abl* cells might be an effect related to inhibition of *v-Abl* as opposed to G1 arrest per se. To test this notion, we used the cyclin-dependent kinase 4,6 inhibitor PD0332991 as an independent means of G1 arrest (34) (Fig. S7). We then assessed clonogenic survival of irradiated WT, PAXX$^{-/-}$, XLF$^{-/-}$, XLF$^{-/-}$PAXX$^{-/-}$, and Ku70$^{-/-}$ *v-Abl* cells that were G1 synchronized with PD0332991 and subsequently released from G1 arrest after irradiation. Similar to observations in STI-571–treated Ku70$^{-/-}$ *v-Abl* cells, PD0332991 treatment of Ku70$^{-/-}$ *v-Abl* cells also induced a profound hypersensitivity under these conditions (Fig. 4*D*). Moreover, similar to observations with STI-571 treatment, PD0332991-treated XLF$^{-/-}$PAXX$^{-/-}$ cells exhibited

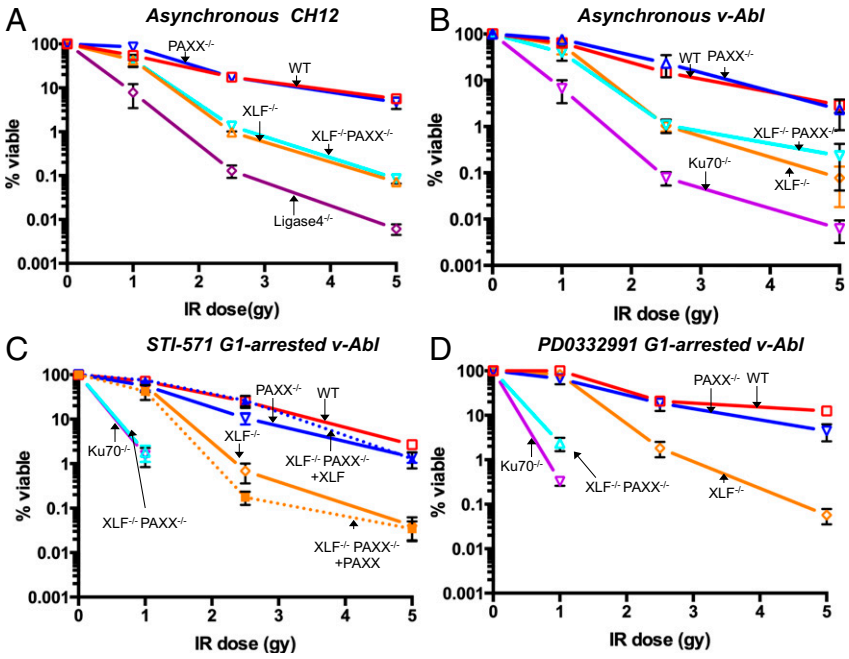

Fig. 4. PAXX provides G1 phase-specific compensation for XLF in cellular resistance to ionizing radiation. Asynchronous CH12 and *v-Abl* lines and G1-arrested *v-Abl* cell lines were subjected to different doses of ionizing radiation and serially diluted to assess clonogenic survival (*Materials and Methods*). In some cases, clonal growth was below the detection of our assay and thus, is not plotted. (*A*) Asynchronous WT ($n = 5$; red), PAXX$^{-/-}$ ($n = 10$; two clones; blue), XLF$^{-/-}$ ($n = 8$; two clones; orange), XLF$^{-/-}$PAXX$^{-/-}$ ($n = 8$; two clones; light blue), and Ligase4$^{-/-}$ ($n = 5$; purple) CH12 cells. (*B*) Asynchronous *v-Abl* cell genotypes are indicated: WT ($n = 7$; red), PAXX$^{-/-}$ ($n = 8$; two clones; blue), XLF$^{-/-}$ ($n = 4$; orange), XLF$^{-/-}$PAXX$^{-/-}$ ($n = 8$; two clones; light blue), and Ku70$^{-/-}$ ($n = 7$; purple) *v-Abl* cells. (*C*) STI-571 G1-arrested genotypes are indicated: WT ($n = 7$), PAXX$^{-/-}$ ($n = 9$; two clones), XLF$^{-/-}$ ($n = 4$), XLF$^{-/-}$PAXX$^{-/-}$ ($n = 8$; two clones), and Ku70$^{-/-}$ ($n = 8$). Retrovirally complemented 3xFLAG-XLF ($n = 5$; blue dashed line) or 3xFLAG-PAXX ($n = 5$; orange dashed line) in XLF$^{-/-}$PAXX$^{-/-}$ and STI-571 G1-arrested *v-Abl* cells is indicated. (*D*) PD0332991 G1-arrested pro–B-cell genotypes are indicated: WT ($n = 3$), PAXX$^{-/-}$ ($n = 3$), XLF$^{-/-}$ ($n = 3$), XLF$^{-/-}$PAXX$^{-/-}$ ($n = 3$), and Ku70$^{-/-}$ ($n = 3$). Mean ± SEM plotted for each ionizing radiation dose. IR, ionizing radiation.

a marked hypersensitivity relative to similarly treated XLF$^{-/-}$ cells (Fig. 4*D*). Thus, using two independent methods of G1 arrest, our results indicate that the observed functional redundancy for PAXX and XLF is, indeed, because of a G1-phase enrichment. We conclude that the functional redundancy between XLF and PAXX in *v-Abl* lines extends to the joining of more general DNA DSBs but is only manifested in G1 phase-enriched cells.

Given the results from V(D)J recombination and ionizing radiation sensitivity assays, we tested whether our findings might result from differential expression levels of PAXX in cycling vs. G1-arrested *v-Abl* cells. For this purpose, we used Western blotting to assay relative PAXX protein levels in cycling WT *v-Abl* cells vs. WT *v-Abl* cells arrested in G1 via treatment with PD0332991 (Fig. S8). These analyses revealed no marked differences in relative PAXX protein levels between the two populations. In this regard, although differential PAXX proteins levels do not seem to explain the increased ionizing radiation sensitivity of G1-arrested vs. cycling cells, PAXX posttranslational modifications and subcellular localization are among many other conceivable mechanisms that could contribute to explaining this phenomenon.

Discussion

We find that PAXX is dispensable for repair of V(D)J recombination-associated DSBs in G1-enriched *v-Abl* cells, repair of *IgH* CSR DSBs in cycling CH12 cells, and mediating normal resistance to ionizing radiation in cycling cells. However, we further find that PAXX is strictly required in the absence of XLF to join V(D)J recombination-associated DSBs in G1-enriched *v-Abl* cells. Likewise, PAXX deficiency greatly increases the ionizing radiation sensitivity of XLF-deficient G1-enriched *v-Abl* cells. These findings provide clear evidence to strongly support the prior conclusion that PAXX functions as a C-NHEJ factor (22, 23) and further show that PAXX is capable of mediating core C-NHEJ functions. Notably, the synthetic defects associated with combined PAXX and XLF deficiencies are manifested only in the context of DSBs generated in XLF$^{-/-}$PAXX$^{-/-}$, G1 phase-enriched *v-Abl* pro-B cells. Although more work will be required to understand why the synthetic core C-NHEJ function conferred by XLF and PAXX has, thus far, manifested only in G1-arrested *v-Abl* pro-B cells, the differential expression of compensatory activities in cycling vs. G1 cells is one possibility. We do note that the ionizing radiation sensitivity phenotype of the XLF$^{-/-}$PAXX$^{-/-}$, G1 phase-enriched *v-Abl* pro-B cells was observed after these cells were released from their G1 block. In this regard, we speculate that, in the absence of PAXX and XLF, ionizing radiation treatment leads to high levels of unrepaired genomic DSBs in the G1-arrested cells that would normally be repaired by core C-NHEJ and that such DSBs may overwhelm the G1 DSB checkpoint that would likely be engaged on release (35), resulting in widespread apoptotic death of released cells.

No *IgH* chromosome breaks accumulated in activated PAXX$^{-/-}$ CSR-stimulated CH12 cells, showing that PAXX is not required for end joining during CSR. In contrast, substantially increased levels of such breaks accumulated in XLF$^{-/-}$ CH12 cells, confirming the requirement for XLF in CSR end joining (14). In this regard, we find that XLF deficiency in CH12 cells has a similar impact to Ligase4 deficiency or other core C-NHEJ factor deficiencies (31, 32) on CSR with respect to both the overall decrease in class switching levels and the greatly increased MH use in CSR junctions between different S regions. In the latter context, it has been noted that S regions may be better substrates for such highly MH-biased joining because of their highly repetitive structure and being resection-prone (30). Overall, based on the two types of assays outlined above, XLF seems to provide functions associated with core C-NHEJ factors, at least in some aspects of CSR. However, we

note the potential caveat in this interpretation, discussed above, regarding the divergence in relative levels of *IgH* chromosome breaks that accumulate in CSR-activated XLF$^{-/-}$ vs. Ligase4$^{-/-}$ CH12 cells. Finally, it is notable that XLF deficiency alone does not have as severe an impact on other processes that use DSB repair via C-NHEJ [e.g., V(D)J recombination and ionizing radiation resistance] as it does on *IgH* class switching. In this regard, compensation for XLF DSB repair functions by PAXX, ATM, and even factors, such as RAG2, that are not considered DSB repair factors clearly obviates a strict requirement for XLF for DSB joining in some of these contexts (16, 20) Whatever the case, it is notable that PAXX is not functionally redundant with ATM for V(D)J recombination. In this regard, PAXX and ATM may have distinct overlapping activities with respect to XLF functions, or alternatively, PAXX may operate downstream of ATM with respect to V(D)J recombination.

Prior studies have shown that PAXX is required for repair of ionizing radiation-induced DSBs in human and chicken cells (22, 23). In this context, our findings that the PAXX-deficient lymphoid cell lines that we studied are not detectably impaired for V(D)J recombination and *IgH* CSR and also, when cycling, do not show increased ionizing radiation sensitivity were unexpected. However, such apparently divergent findings may reflect differences in the types of assays used and/or differences in the contribution of PAXX to particular joining pathways in the cell types analyzed. As one example of the latter possibility, XLF-deficient mouse embryonic fibroblasts (MEFs) and ES cells have a markedly greater defect in end joining of V(D)J recombination substrates compared with WT MEFs or ES cells when assayed with ectopically introduced episomal V(D)J recombination substrates (14). Likewise, in XLF-deficient *v-Abl* pro-B cells, there is a greater defect in V(D)J joining within chromosomally integrated as opposed to episomal V(D)J recombination substrates (14). In any case, based on our current findings, we would predict that PAXX$^{-/-}$ mice will be competent for V(D)J recombination and CSR and that XLF$^{-/-}$PAXX$^{-/-}$ mice will likely have an SCID phenotype because of inability to join V(D)J recombination-associated DSBs. Finally, it is also conceivable that variations in PAXX activity might contribute to the variable immunodeficiency phenotype observed in XLF-deficient humans (6, 14, 16).

Materials and Methods

Chromosomal V(D)J Recombination Assays. *v-Abl* lines (details on gRNAs used for line generation are in Table S2) containing the pMX-DEL-CJ, pMX-DEL-SJ, or pMX-INV cassettes (26) underwent V(D)J recombination and are described in *SI Materials and Methods*.

CH12 CSR, *IgH* Metaphase FISH, and LAM-HTGTS. CH12 cells underwent CSR as previously described (36); *IgH* metaphase FISH has been previously described (28). Junction structure analysis of IgH S regions using LAM-HTGTS has been described previously (30). Additional details are provided in *SI Materials and Methods*.

Clonogenic Ionizing Radiation Sensitivity Assays. Clonogenic survival of *v-Abl* and CH12 cells after ionizing radiation treatment is described in *SI Materials and Methods*.

ACKNOWLEDGMENTS. We thank Pankaj Mandal and Derrick Rossi for providing the cyclin-dependent kinase 4,6 inhibitor for G1 arrest studies. We thank members of the laboratory of Peter Sicinski for advice on cyclin blots and the gift of the cyclin A2 antibody. We thank Kefei Yu for providing the Lig4-pMSCV-puro plasmid and Ligase4$^{-/-}$ CH12 cells (designated clone 1) for these studies. We thank Ming Tian for helpful advice and comments on the ionizing radiation sensitivity assays, Monica Gostissa for help with cytogenetic assays, Feilong Meng for help with CRISPR-Cas9 deletion in cell lines, Rohit Panchakshari for helping to map the breakpoint on the CH12 non-coding allele, Cristian Boboila for generating the Ku70$^{-/-}$ *v-Abl* cells, Bjoern Schwer for general advice on end joining assays in CH12 cells, and the rest of the laboratory of F.W.A. for critical feedback and support. This work was supported by NIH Grants AI0200047 and AI1077595. V.K. is supported by NIH Ruth L. Kirchstein National Research Service Award Fellowship F30CA189740-02. F.W.A. is an investigator with the Howard Hughes Medical Institute.

1. Orthwein A, et al. (2015) A mechanism for the suppression of homologous recombination in G1 cells. *Nature* 528(7582):422–426.
2. Takata M, et al. (1998) Homologous recombination and non-homologous end-joining pathways of DNA double-strand break repair have overlapping roles in the maintenance of chromosomal integrity in vertebrate cells. *EMBO J* 17(18):5497–5508.
3. Rothkamm K, Krüger I, Thompson LH, Löbrich M (2003) Pathways of DNA double-strand break repair during the mammalian cell cycle. *Mol Cell Biol* 23(16):5706–5715.
4. Mills KD, et al. (2004) Rad54 and DNA Ligase IV cooperate to maintain mammalian chromatid stability. *Genes Dev* 18(11):1283–1292.
5. Alt FW, Zhang Y, Meng F-L, Guo C, Schwer B (2013) Mechanisms of programmed DNA lesions and genomic instability in the immune system. *Cell* 152(3):417–429.
6. Kumar V, Alt FW, Oksenych V (2014) Functional overlaps between XLF and the ATM-dependent DNA double strand break response. *DNA Repair (Amst)* 16:11–22.
7. Desiderio S (2010) Temporal and spatial regulatory functions of the V(D)J recombinase. *Semin Immunol* 22(6):362–369.
8. Schatz DG, Swanson PC (2011) V(D)J recombination: Mechanisms of initiation. *Annu Rev Genet* 45(1):167–202.
9. Hwang JK, Alt FW, Yeap LS (2015) Related mechanisms of antibody somatic hypermutation and class switch recombination. *Microbiol Spectr* 3(1):MDNA3-0037-2014.
10. Boboila C, Alt FW, Schwer B (2012) *Classical and Alternative End-Joining Pathways for Repair of Lymphocyte-Specific and General DNA Double-Strand Breaks* (Elsevier, Amsterdam), 1st Ed.
11. Schwer B, et al. (2016) Transcription-associated processes cause DNA double-strand breaks and translocations in neural stem/progenitor cells. *Proc Natl Acad Sci USA* 113(8):2258–2263.
12. Wei P-C, et al. (2016) Long neural genes harbor recurrent DNA break clusters in neural stem/progenitor cells. *Cell* 164(4):644–655.
13. Ma Y, Pannicke U, Schwarz K, Lieber MR (2002) Hairpin opening and overhang processing by an Artemis/DNA-dependent protein kinase complex in nonhomologous end joining and V(D)J recombination. *Cell* 108(6):781–794.
14. Li G, et al. (2008) Lymphocyte-specific compensation for XLF/cernunnos end-joining functions in V(D)J recombination. *Mol Cell* 31(5):631–640.
15. Vera G, et al. (2013) Cernunnos deficiency reduces thymocyte life span and alters the T cell repertoire in mice and humans. *Mol Cell Biol* 33(4):701–711.
16. Zha S, et al. (2011) ATM damage response and XLF repair factor are functionally redundant in joining DNA breaks. *Nature* 469(7329):250–254.
17. Oksenych V, et al. (2012) Functional redundancy between repair factor XLF and damage response mediator 53BP1 in V(D)J recombination and DNA repair. *Proc Natl Acad Sci USA* 109(7):2455–2460.
18. Liu X, et al. (2012) Overlapping functions between XLF repair protein and 53BP1 DNA damage response factor in end joining and lymphocyte development. *Proc Natl Acad Sci USA* 109(10):3903–3908.
19. Oksenych V, et al. (2013) Functional redundancy between the XLF and DNA-PKcs DNA repair factors in V(D)J recombination and nonhomologous DNA end joining. *Proc Natl Acad Sci USA* 110(6):2234–2239.
20. Lescale C, et al. (2016) RAG2 and XLF/Cernunnos interplay reveals a novel role for the RAG complex in DNA repair. *Nat Commun* 7:10529.
21. Corneo B, et al. (2007) Rag mutations reveal robust alternative end joining. *Nature* 449(7161):483–486.
22. Ochi T, et al. (2015) DNA repair. PAXX, a paralog of XRCC4 and XLF, interacts with Ku to promote DNA double-strand break repair. *Science* 347(6218):185–188.
23. Xing M, et al. (2015) Interactome analysis identifies a new paralogue of XRCC4 in non-homologous end joining DNA repair pathway. *Nat Commun* 6:6233.
24. Craxton A, et al. (2015) XLS (c9orf142) is a new component of mammalian DNA double-stranded break repair. *Cell Death Differ* 22(6):890–897.
25. Roy S, et al. (2015) XRCC4/XLF interaction is variably required for DNA repair and is not required for ligase IV stimulation. *Mol Cell Biol* 35(17):3017–3028.
26. Bredemeyer AL, et al. (2006) ATM stabilizes DNA double-strand-break complexes during V(D)J recombination. *Nature* 442(7101):466–470.
27. Nakamura M, et al. (1996) High frequency class switching of an IgM+ B lymphoma clone CH12F3 to IgA+ cells. *Int Immunol* 8(2):193–201.
28. Franco S, et al. (2006) H2AX prevents DNA breaks from progressing to chromosome breaks and translocations. *Mol Cell* 21(2):201–214.
29. Franco S, et al. (2008) DNA-PKcs and Artemis function in the end-joining phase of immunoglobulin heavy chain class switch recombination. *J Exp Med* 205(3):557–564.
30. Dong J, et al. (2015) Orientation-specific joining of AID-initiated DNA breaks promotes antibody class switching. *Nature* 525(7567):134–139.
31. Yan CT, et al. (2007) IgH class switching and translocations use a robust non-classical end-joining pathway. *Nature* 449(7161):478–482.
32. Boboila C, et al. (2010) Alternative end-joining catalyzes class switch recombination in the absence of both Ku70 and DNA ligase 4. *J Exp Med* 207(2):417–427.
33. Han L, Yu K (2008) Altered kinetics of nonhomologous end joining and class switch recombination in ligase IV-deficient B cells. *J Exp Med* 205(12):2745–2753.
34. Turner NC, et al.; PALOMA3 Study Group (2015) Palbociclib in hormone-receptor-positive advanced breast cancer. *N Engl J Med* 373(3):209–219.
35. Chen J (2016) The cell-cycle arrest and apoptotic functions of p53 in tumor initiation and progression. *Cold Spring Harb Perspect Med* 6(3):a026104–a026116.
36. Boboila C, et al. (2012) Robust chromosomal DNA repair via alternative end-joining in the absence of X-ray repair cross-complementing protein 1 (XRCC1). *Proc Natl Acad Sci USA* 109(7):2473–2478.
37. Gibson DG, et al. (2009) Enzymatic assembly of DNA molecules up to several hundred kilobases. *Nat Methods* 6(5):343–345.